PET and SPECT imaging for the acceleration of anti-cancer drug development

Christopher RT Hillyar[1], James C. Knight[1], Katherine A. Vallis[1], Bart Cornelissen[1†]

[1]*CRUK/MRC Oxford Institute for Radiation Oncology, University of Oxford, Oxford, United Kingdom*

Word count: 5,365 words excluding references and figures

The authors disclose no potential conflicts of interest.

[†] To whom correspondence should be addressed:
Dr. Bart Cornelissen
CRUK/MRC Oxford for Radiation Oncology
Department of Oncology
University of Oxford
Old Road Campus Research Building
Off Roosevelt Drive
Oxford OX3 7LJ
Tel: +44 (0)1865 857126
Fax: +44 (0)1865 857127
Email: bart.cornelissen@oncology.ox.ac.uk

1. Abstract

Lead-compound optimization is an iterative process in the cancer drug development pipeline, in which small molecule inhibitors or biological compounds that are selected for their ability to bind specific targets are synthesised, tested and optimised. This process can be accelerated significantly using molecular imaging with nuclear medicine techniques, which aim to monitor the biodistribution and pharmacokinetics of radiolabelled versions of compounds. Positron emission tomography (PET) and single-photon emission computed tomography (SPECT) can be used to quantify four-dimensional (temporal and spatial) clinically relevant information, to demonstrate tumor uptake of, and monitor the response to treatment with lead-compounds. This review discusses the pre-clinical and clinical value of the information provided by nuclear medicine imaging compared to the histological analysis of biopsied tissue samples. Also, the role of nuclear medicine imaging is discussed with regard to the assessment of the treatment response, radiotracer biodistribution, tumor accumulation, toxicity, and pharmacokinetic parameters, with mention of microdosing studies, pre-targeting strategies, and pharmacokinetic modelling.

Key words: PET, SPECT, cancer, biodistribution, drug delivery, microdosing, pretargeting, kinetic imaging.

2. Introduction

The birth of medical imaging is attributed to the German physicist Wilhelm Conrad Röntgen, who, in 1895 discovered ‘a new kind of ray’ and publically produced the very first radiograph, featuring the hand of the prominent Swiss professor of anatomy Rudolf Albert von Kölliker [1]. Since the discovery of the X-ray (Röntgen used X to denote the unknown), medical imaging has advanced such that it now encompasses the use of ionising and non-ionising electromagnetic radiation, both visible and invisible, and radiowaves and soundwaves. Medical imaging modalities include planar X-ray imaging, magnetic resonance imaging (MRI), computed tomography (CT), optical techniques, ultrasound imaging, positron emission tomography (PET), and single-photon emission computed tomography (SPECT).

Modern nuclear medicine imaging involves the four-dimensional detection (temporally and spatially in three-dimensions) of molecular targets within an organ of interest or malignant tissue. Major advances in the field of cancer research have been made using PET or SPECT imaging, which have enabled the detection of a wide range of disease biomarkers. Both PET and SPECT detect radioactive compounds administered to animals or human patients. PET detects mono-energetic photons (511 keV) emitted in opposite directions resulting from the annihilation of a positron emitted by such radioisotopes as ^{11}C, ^{13}N, ^{15}O, ^{18}F, and ^{89}Zr. In contrast, SPECT imaging detects a spectrum of gamma photon emissions from such radioisotopes as ^{99m}Tc, ^{123}I, ^{131}I, and ^{111}In.

Small-animal PET and SPECT imaging is an established paradigm for proof-of-principle studies which demonstrate the pharmacokinetics of novel radiotracers, as well as the ability of a radiotracer to detect disease biomarker expression in malignant tissue and monitor therapeutic response. Thus, PET and SPECT are essential pre-clinical research tools for the acceleration of the drug development pipeline [2]. In the pre-clinical setting and in the oncology clinic, PET or SPECT are routinely co-registered with CT or MRI [3, 4].

This aim of this review is to discuss the pre-clinical and clinical value of the information provided by nuclear medicine imaging compared to the histological analysis of biopsied tissue samples. Also, the role of nuclear medicine imaging is discussed with regard to the assessment of treatment response, radiotracer biodistribution, tumor accumulation, toxicity,

and pharmacokinetic parameters, with mention of microdosing studies, pre-targeting strategies, and pharmacokinetic modelling.

3. The pre-clinical and clinical value of PET or SPECT imaging

Nuclear medicine imaging based on PET or SPECT aims to provide information of diagnostic and prognostic value that can be used to predict the outcome of cancer treatment. The features of PET and SPECT are summarized in Table 1. The main advantage of PET is its high sensitivity (10^{-11}-10^{-12} mol/l), while SPECT is more widely established and uses radioisotopes that are relatively long-lived, inexpensive and generally more readily available. In the clinic, PET and SPECT imaging can provide information about the location, volume and heterogeneity of primary and secondary cancer sites, and therefore reduce the number of inappropriate explorative or diagnostic surgical procedures that are performed during tumor diagnosis, staging and management.

Nuclear medicine imaging studies rely on the production and availability of radiotracers that target disease biomarkers or biological components. A wide range of radiotracers have been developed that target growth factor receptors [5, 6], signaling components [7], markers of apoptosis [8], proliferation markers [9], proteolytic enzymes [10], tumor neovasculature [11], extracellular matrix proteins [10], and molecular antigens inside cells [12]. Biomarkers of disease have become increasingly useful in the evaluation of clinical and translational cancer research. The development of imaging biomarkers using radiotracers is therefore, aimed at making significant improvements in the management of malignant disease.

Radiotracers that detect metabolic processes include ^{18}F-FDG (^{18}F-labelled deoxy-glucose) and ^{18}F-FLT (^{18}F-labelled deoxy-thymidine), which can be used to image glucose metabolism and cell proliferation, respectively [13]. Several metabolic radiotracers serve as substrates for amino acid transporters: these include ^{18}F-FDOPA (^{18}F-labelled L-DOPA), ^{18}F-FET (^{18}F-labelled ethyl-tyrosine), ^{123}I-IMT (^{123}I-labelled α-methyl-tyrosine), ^{11}C-MET (^{11}C-labelled methionine), and ^{18}F-FMT (^{18}F-labelled methyl-D-tyrosine) [14]. Apoptosis has been imaged using radiolabelled derivatives of Annexin V, a naturally occurring ligand of phosphatidylserine expressed on the outer leaflet of the surface membrane by apoptotic cells [8]. Caspases, the proteolytic enzymes that cleave intracellular proteins and DNA during apoptosis, have also been targeted with radiotracers to image apoptosis [15, 16].

Various strategies have been developed to image signalling networks implicated in tumorigenesis, at different levels in the cell signalling cascades. Radiotracers have been developed that target upstream signalling components such as EGFR, which is commonly overexpressed in breast cancer [17]. Other radiotracers have been developed to target receptors associated with signalling components that regulate angiogenesis, such as VEGF/VEGFR [18], integrin $\alpha_V\beta_3$ [19], Ephrin [20], c-Met [21] and PDGFR [22]. Downstream signaling components, such as hypoxia inducible factor-1 (HIF-1), have also been targeted with radiotracers and imaged using PET [23]. Radiotracers that target signalling components such as these may have clinical application in the stratification of patients and the assessment of the treatment response [24, 25].

The hallmarks of cancer are acquired during oncogenesis through a multistep process that involves the sequential acquisition of genetic mutations that cause the inappropriate expression or activation of oncoproteins, or the loss of function of tumor suppressor proteins [26]. These genetic and proteomic changes collaborate to drive cellular and physiological changes associated with a malignant disease phenotype. ^{18}F-FDG and ^{18}F-FLT are excellent examples of radiotracers that can be used to image the physiological phenotypes that arise as the ultimate expression of the acquisition of the hallmarks of cancer, i.e. aberrant glucose metabolism and unlimited replicative potential, respectively. Molecularly targeted radiotracers can also be used to indirectly image the genetic changes that occur in the early stages of tumor initiation and progression, which result in, e.g., the overexpression of oncogenes [27], the stabilization of (inactive forms of) tumor suppressor proteins, or the phosphorylation (activation) of DNA damage repair proteins [12, 28]. Molecular imaging can also be used to measure the changes at the molecular level that result in the overexpression of the oncoproteins or tumor suppressor proteins. Thus, nuclear medicine imaging can be used to assess the response to molecularly targeted or chemotherapeutic agents that, directly or indirectly, influence the molecular, cellular and physiological changes associated with tumorigenesis [29].

Although PET and SPECT can only be used to measure molecular or metabolic processes through the detection of radiotracers that are injected into small animals or human patients, they do not provide detailed anatomical information. Thus, ^{18}F-FDG-PET imaging can detect glycolytic rate with high sensitivity, but the PET image suffers from poor spatial resolution.

In oesophageal cancer, a threshold of 5 mm is routinely applied to ^{18}F-FDG avidity in a PET image to identify malignant from benign lesions [30]. To overcome the limitations of poor spatial resolution of, and lack of anatomical information that is provided by the detection of radiotracers, PET or SPECT can be co-registered with CT or MRI. Routine CT or MRI co-registration provides detailed anatomical information, which enhances the diagnostic and prognostic value of the PET or SPECT images. Thus, PET and SPECT images fused with CT or MRI images show disease biomarkers within the context of the detailed anatomy of the whole body which enhances the diagnostic information obtained by fusion imaging [31].

Anatomically co-registered PET/CT images are more sensitive than CT or MRI at differentiating malignant from benign lesions [3, 4]. In the clinic, whole body ^{18}F-FDG-PET/CT is an invaluable tool for the detection of metastatic lesions [32]. The recent introduction of PET/MRI (MRI being the modality of choice for imaging soft tissue structures) will also have a major role in the diagnosis, treatment planning and assessment of brain tumors in the future, especially where the anatomy of the brain makes surgical biopsy undesirable or impossible [33]. In comparison, SPECT/CT has been shown to differentiate malignant from benign radiotracer distributions [34]. Thus, the additional anatomical information provided by the CT component of PET/CT adds significant value to diagnostic procedures and treatment planning [35].

4. Molecular imaging versus histological analysis

The effort to develop non-invasive molecular imaging using PET and SPECT has been driven by the need for clinically relevant diagnostic and prognostic information. These techniques can complement the information provided by histological analysis, which involves the microscopic examination and subjective classification of chemical staining of tissue from a limited number of consecutive biopsies of normal and malignant tissue. Histological analysis can provide important information regarding the expression of a protein or subcellular structure relating to disease, cell shapes and tissue distributions.

In contrast, molecular imaging can be used to measure the number of molecules in low capacity systems, such as the number of receptors on the cell membranes of tumor cells. In addition to molecular imaging, PET and SPECT metabolic imaging aims to measure metabolic processes, such as glycolytic rate using ^{18}F-FDG; while functional imaging

measures blood flow, oxygen consumption and other functionalities. Medical imaging approaches such as these provide information about the biodistribution of a systemically injected radiotracer [36]. This offers an alternative to invasive sampling techniques, such as fine-needle aspiration, core needle biopsy, vacuum-assisted biopsy or image guided biopsy, that may interfere with the gross anatomy and fine structure of a tumor during the time-course of a small-animal study or human trial. Medical imaging also does not suffer from artefacts induced by improper fixation, poor dehydration, paraffin infiltration or poor sectioning, which may occur even when sample preparation is performed by experienced technicians or automated robotic systems.

Tumor heterogeneity and clonal evolution within malignant tissue can be assessed to a limited extent through multi-region tissue sampling with whole genome sequencing [37]. This provides information about the different mutations that are present in hundreds of genes in different regions of a primary tumor or at different sites of metastasis. In contrast, PET imaging provides information about the total amount and heterogeneity of uptake of a radiotracer within a region of interest in an organ or malignant site throughout the whole animal or patient.

5. Monitoring the response to anti-cancer therapeutics

5.1. Imaging glycolytic rate with ^{18}F-FDG

In the clinical setting, ^{18}F-FDG is the most widely used radiotracer for PET imaging. Assessment of glycolytic rate using ^{18}F-FDG is an established technique in clinical practice that is used routinely for tumor staging, the assessment of the response to therapy, and the identification of recurrent disease in a wide range of malignancies, including lymphoma, non-small-cell lung cancer, head and neck cancer, and colorectal cancer [29]. ^{18}F-FDG is a deoxyglucose analogue (2-deoxy-2-[^{18}F]fluoro-D-glucose) that has been used most extensively in PET imaging to assess the effect of chemotherapeutic agents on glucose metabolism [38-46]. Upregulated glucose transporters on tumor cells are responsible for the translocation of ^{18}F-FDG to the intracellular compartment, where ^{18}F-FDG is phosphorylated by hexokinase to form ^{18}F-FDG-6-phosphate. Unlike glucose-6-phosphate, ^{18}F-FDG-6-phosphate does not progress further through the glycolytic pathway. Therefore, ^{18}F-FDG-6-phosphate rapidly accumulates inside metabolically active tumor cells, which commonly

show increased glucose transporter expression, enhanced hexokinase activity, and modified glucose metabolism (the Warburg effect) [47].

Chemotherapeutic agents such as nitrogen mustards and antifolate drugs were firstly used in the 1940s [48]. Since, the range of chemotherapeutics that have been used in the clinic, has expanded to include anti-metabolites (e.g. methotrexate, 5-fluorouracil, thiopurines), anti-tumor antibiotics (e.g. doxycycline), platinum-based compounds (e.g. cisplatin), and vinca alkaloids (e.g. vincristine) [49]. Chemotherapeutics act, in general, by inhibiting DNA synthesis, protein synthesis or the action of the mitotic spindle, thereby reducing the proliferative potential of replicating cells. Within a highly proliferative tumor cell population, chemotherapeutics cause the total number of metabolically active tumor cells to shrink by reducing the number of cells that survive successive rounds of cell division. As a consequence, the total uptake of ^{18}F-FDG in the tumor is reduced. The reduction in ^{18}F-FDG avidity in an ^{18}F-FDG-PET image that accompanies reduced ^{18}F-FDG tumor uptake is a quantifiable effect that can be used as a surrogate measure of the efficacy of, and tumor response to chemotherapeutic treatments. Quantification with PET imaging utilizes the standardized uptake value (SUV): the SUV_{mean} is the radiotracer avidity per pixel expressed as an average avidity over all the pixels included in the region of interest (ROI) of the tumor or organ of interest, while the SUV_{max} is the highest radiotracer avidity of any pixel within the ROI.

Several studies have established a role for ^{18}F-FDG-PET imaging in the pre-clinical setting as a method for predicting the efficacy of chemotherapeutic agents for subsequent use in human patients [38-46, 50]. For example, in a recent study by Jensen *et al*. mice bearing human ovarian cancer xenografts (A2780) were treated with a combination of carboplatin (40 mg/kg i.p.) and paclitaxel (10 mg/kg i.v.) [51]. Mice were treated on days 0 and 5 and the tumor response to chemotherapy was monitored by ^{18}F-FDG-PET imaging on days 1, 4, and 8. On day 4, the tumor xenografts in mice treated with the combination therapy had a significantly lower SUV_{max} for ^{18}F-FDG compared to a control population of untreated mice (105±4% and 138±9%, respectively; P=0.002).

In another study by Mudd *et al.,* ^{18}F-FDG-PET imaging was used to assess the response of a murine model of human non-small cell lung cancer (Calu-6) to treatment with linifanib (ABT-869), a small molecule inhibitor of the tyrosine kinase modules of the vascular

endothelial growth factor receptor (VEGFR) and platelet derived growth factor receptor (PDGFR) [46]. Linifanib (12.5 mg/kg) was administered orally twice a day for 7 days and PET imaging was performed on days -1, 1, 3, and 7. Compared to a vehicle-treated group, reduced ^{18}F-FDG uptake was observed as early as 1 day after starting treatment with linifanib (Fig. 1), and a significant reduction was observed in all subsequent PET scans. Thus, ^{18}F-FDG-PET imaging is a sensitive method that can be used to show changes in glycolytic rate in response to anti-cancer treatment with chemotherapeutic agents.

However, it needs to be noted that ^{18}F-FDG imaging needs to be treated with care, as it is often used unnecessarily, without regard to the mechanism of the therapeutic response. It is important to match the specific biological mechanism of cancer drugs to an accompanying imaging biomarker, and ^{18}F-FDG imaging may not always be the most appropriate. A recent study by Alvarez *et al*. highlighted this concern, when they concluded that it is the particular oncogenic pathways(s) that become activated within each individual tumor that is the primary determinant of glycolytic enzyme-mediated ^{18}F-FDG uptake [52]. It, therefore, would provide more clinically relevant information if future imaging studies were directed at detecting the activation of the components of the oncogenic pathways upstream of ^{18}F-FDG uptake.

5.2. Imaging tumor delivery of anti-cancer antibodies

Antibody therapy for cancer has been established over the past two decades. A wide variety of antibody constructs are potentially available for targeted anti-cancer treatment. These include intact IgG (CD20, CD33, EGFR, HER2, VEGF), IgE and IgM (GM2), bispecific antibodies (CD19-CD3, EPCAM-CD3, gp100-CD3), protein-Fc (angiopoietin 1/2, VEGFR1/2), minibodies (CEA, ERBB2), affibodies (ERBB2), diabodies (TAG-72), and scFv (CC49, ERBB2) [53]. Two important examples of anti-cancer antibodies include trastuzumab (Herceptin) and bevacizumab (Avastin). Herceptin is a humanized, monoclonal IgG1κ antibody that is used to specifically inhibit the induction of growth signals by the growth factor receptor HER2/neu, which is overexpressed by, and which confers a poorer outcome for 25-30% of human breast cancers [54]. In contrast, Avastin is a VEGFA-specific, humanized, monoclonal IgG1κ antibody that is used as an anti-angiogenic therapeutic. VEGFA is a member of the larger VEGF family, which includes pro- and anti-angiogenic proteins. Tumor cells secrete VEGFA, which is an endothelial cell-specific mitogen, to

promote angiogenesis [55]. In several studies, radiolabelled versions of these anti-cancer antibodies have been used to image the biodistribution and tumor delivery of the non-radiolabelled antibodies. The same principles may be applied to the ever increasing legion of antibody drug conjugates [56].

5.2.1. Trastuzumab

Since original FDA approval of Herceptin for the treatment of late-stage HER2-positive breast cancer, trastuzumab has been radiolabelled with ^{68}Ga and ^{89}Zr for PET imaging, and ^{111}In for SPECT imaging, to predict the tumor delivery of Herceptin to HER2-overexpressing tumors [57-63]. A first-in-human clinical study using ^{89}Zr-labelled trastuzumab-PET imaging showed excellent radiotracer uptake in HER2-positive tumors [64]. In the pre-clinical setting, PET imaging using ^{89}Zr-labelled trastuzumab has been shown to detect down-regulation of HER2 expression in response to treatment of a xenograft model of human gastric cancer with afatinib, a small molecule inhibitor of EGFR and HER2 [65]. SPECT imaging of trastuzumab-mediated HER2-downregulation has also been shown to be feasible, in murine models of breast cancer, using an ^{111}In-labelled version of pertuzumab, an alternative anti-HER2 antibody [66]. Radiolabelled HER2-binding affibodies have also been extensively used for the quantification of drugs that influence HER2 expression, such as the HSP90 inhibitor 17-allylamino-geldanamycin [67].

However, the tumor uptake of ^{111}In-labelled trastuzumab was demonstrated by McLarty *et al.* not to correlate with tumor expression of HER2 using SPECT imaging [68]. Correcting ^{111}In-labelled trastuzumab avidity for circulating radioactivity and tumor accumulation of polyclonal IgG (i.e. non-specific, passive antibody uptake due to the enhanced permeability and retention effect [69], that was not dependent on tumor expression of HER2) was used to show associations between ^{111}In-labelled trastuzumab avidity and tumor expression of HER2. Using this approach, McLarty *et al.* found a clear nonlinear association between ^{111}In-labelled trastuzumab avidity and tumor expression of HER2 for a number of mouse models of human breast cancer (MDA-MB-231, BT-474$_{HET}$, BT-20, MDA-MB-361, and MCF7/HER2-18). The same group also found that ^{18}F-FDG-PET imaging was able to effectively predict the efficacy of trastuzumab, by differentiating trastuzumab-responsive from -unresponsive human breast cancer xenografts in athymic mice [70].

Finally, SPECT imaging has also been used to predict the biodistribution and toxicity profile of trastuzumab. In a study by Behr *et al.*, seven of 20 patients treated with a regimen of trastuzumab were found using SPECT imaging to have myocardial uptake of ^{111}In-labelled trastuzumab. Six of these patients developed functional class II–IV heart failure (as classified by the New York Heart Association guidelines) after treatment with trastuzumab, and the seventh patient had episodes of cardiac arrhythmia during trastuzumab administration. In the 13 patients without myocardial uptake of ^{111}In-labelled trastuzumab, no adverse cardiac effects occurred [71]. These results, however, were not confirmed by the complementary study of Perik *et al.* [72]. We direct the reader to recent reviews by Milano *et al.* and de Geus-Oei *et al*., which discuss in detail the molecular mechanisms involved and the use of several nuclear medicine imaging agents to monitor cancer treatment-induced cardiac toxicity [73, 74].

5.2.2. Bevacizumab

In the clinic, the antibody bevacizumab can be used as a therapeutic agent with the aim of reducing blood supply and neoangiogenesis in tumors and metastases [75, 76]. Radiolabelled versions of bevacizumab or its antibody fragments have been reported, which included the use of radioisotopes for PET imaging, ^{124}I [77], ^{64}Cu [78], and ^{89}Zr [79]; and, for SPECT imaging, ^{99m}Tc [80] and ^{111}In [81]. Radiolabelled versions of bevacizumab have also been used to monitor the tumor response to anti-cancer therapeutics designed to inhibit angiogenesis. Desar *et al*. used ^{111}In-labelled bevacizumab-SPECT imaging to monitor the effects of a 4-week regimen of sorafenib (Nexavar), and showed a marked reduction in tumor uptake of ^{111}In-labelled bevacizumab [82].

As was the case for radiolabelled trastuzumab, tumor uptake of radiolabelled bevacizumab did not, however, directly correlate with VEGF levels in tumor microenvironment [83-85]. These studies are an important reminder for the requirement of the validation of molecular imaging agents that are designed to molecularly target disease biomarkers. Although the reduced uptake of bevacizumab has been shown to be useful as a diagnostic agent for the monitoring of the tumor response to sorafenib treatment, this result must be treated with a degree of caution when inferring that sorafenib treatment has caused a reduction in VEGF expression in the tumor. Nevertheless, Heskamp *et al.* reported that SPECT/CT imaging revealed that bevacizumab treatment significantly reduced tumor uptake (-40%) of ^{111}In-

labelled cetuximab, an anti-EGFR antibody [86]. In contrast, antiangiogenic treatment with bevacizumab has not been found to alter the uptake of radiolabelled RGD-peptide dimers, which can be used to image integrin $\alpha_v\beta_6$ expression on tumour neovasculature [87]. This latest study again highlights the need for correct validation of combinations of cancer drugs and companion imaging biomarkers.

6. Microdosing studies using radiolabelled small molecules

Radiolabelled versions of small molecule drugs can provide information on *in vivo* characteristics for their non-radiolabelled counterparts and therefore accelerate the drug discovery process. In a seminal PET imaging study, an ^{18}F-labelled version of altanserin, which binds to the 5-HT2A receptor (serotonin receptor), was used with PET imaging to monitor the loss with age of 5-HT2A receptors in the human brain [88]. Neuroimaging studies such as this paved the way for modern radiolabelled small molecule imaging, which can assess metabolite formation, pharmacokinetics, pharmacodynamics, receptor occupancy rate, affinity, and bioavailability of small molecules.

There is high potential for the advancement of radiolabelling in the pharmaceutical industry to drive nuclear imaging of anti-cancer small molecules forward, especially since ^{3}H- and ^{14}C-labelling of small molecules is commonplace. To reduce the proportion of small molecules failing to progress through Phase I or II clinical trials – now estimated to be 40% – the concept of microdosing studies has been introduced to highlight small molecules with inappropriate or unsafe pharmacokinetic and metabolic characteristics [89]. Thus, microdosing studies can accelerate the drug development process and enhance the safety of human clinical trials [90], by providing information on the pharmacokinetics, pharmacodynamics, biodistribution, and tumor uptake, at an earlier stage than testing pharmacological doses in Phase I or II clinical trials.

In a microdosing imaging study, a sub-pharmacological dose (1/100th of the lowest dose established in pre-clinical studies to produce a pharmacological effect) is detected using PET or SPECT. Even at these very low doses (in the low microgram range) the biodistribution is readily detectable *in vivo*, due to the high sensitivity of the instrumentation (PET in particular). After administration of a radiolabelled small molecule, real-time biodistribution data are collected to determine the rate and extent of drug absorption, the residence time in

target and normal organs, as well as routes and rates of drug clearance [91]. Thus, it is possible to predict the pharmacokinetic behaviour of pharmacological doses of small molecules.

^{11}C-labelled docetaxel is an excellent example of microdosing principles (review in Van der Veldt et al. [92]). Van Tilburg *et al*. radiolabel the taxane docetaxel with positron-emitting radionuclide ^{11}C by replacing one of the stable carbon atoms. Only 30 μg of ^{11}C-labelled docetaxel was required for PET imaging, a dose that was 50-fold lower than that required for therapeutic effect (Fig. 2). Microdosimetric imaging was possible, in part, due to the high sensitivity of PET imaging and, in part, due to the relatively high specific activity of ^{11}C that was incorporated into docetaxel. Microdosing imaging studies in rats showed that ^{11}C-labelled docetaxel was cleared from blood and plasma within less than five minutes. Highest ^{11}C-docetaxel uptake was found in spleen, followed by urine, lung and liver, whereas brain and testes showed the lowest uptake [92]. A subsequent microdosing imaging study in humans similarly found rapid clearance from plasma; no radiolabeled metabolites were detected [93]. Consequently, quantification of ^{11}C-docetaxel pharmacokinetics with PET imaging was reproducible in human patients with lung tumors [93, 94].

7. Novel pretargeting approaches in molecular imaging

Pretargeting is a multi-step approach to molecular imaging that aims to reduce radiation exposure in normal tissue and enhance the tumor-to-normal tissue ratio. The technique has recently proven useful to image the drug delivery of a PARP inhibitor to tumor tissue. First, an unlabelled, tumor antigen-specific pretargeting molecule (i.e. an antibody) is administered that localizes within tumor tissue. Second, a relatively small, radiolabelled compound that binds to the pretargeting molecule is administered which rapidly accumulates in the tumor but is cleared from normal tissue within one hour [95]. The radiolabelled compound is administered following a predetermined lag period to allow the pretargeting molecule sufficient time to accumulate in tumor tissue and to be cleared from the circulation and normal tissue [96]. In the clinic, one such pretargeting approach utilises a chemically conjugated F(ab')$_2$ comprising an anti-carcinoembryonic antigen (CEA) Fab' and an anti-EOTUBE Fab', that can be administered four days prior to SPECT imaging with an ^{111}In-labelled hydroxyethylthiourido-derivative of benzyl EDTA (^{111}In-EOTUBE) [97, 98].

Recently, the Weissleder group developed a multi-step radiolabelling process based on a *trans*-cyclooctene (TCO)/tetrazine reaction, which might have future applications in pretargeting strategies. Advantages of TCO/tetrazine reaction-based pretargeting approach include, fast reaction times (6,000 M^{-1} s^{-1}), high selectivity, and the biocompatibility of the reaction conditions. First, a PARP1 inhibitor, AZD2281 (Olaparib), which has nanomolar affinity, was tetrazine-modified. Second, TCO was ^{18}F-labelled away from the cyclooctenyl ring to avoid isomerization to bicyclo[3.3.0]octenes. Third, tetrazine-modified AZD2281 was radiolabelled via bioorthogonal click chemistry with ^{18}F-TCO [99]. This approach produced significantly higher yields of ^{18}F-labelled AZD2281 and in a shorter time compared to the *de novo* synthesis of ^{18}F-AZD2281 by substituting ^{18}F for the aryl fluorine atom.

The feasibility of the TCO/tetrazine system for pretargeting strategies was validated *in vitro* using TCO-modified AZD2281 and fluorophore (Texas Red)-labelled tetrazine. In MDA-MB-436 cells, TCO-AZD2281 assembled with Texas Red-tetrazine and was shown to colocalize with immunochemically stained PARP1 in the nucleus (Fig. 3) [100]. Subsequently, ^{18}F-TCO-tetrazine-AZD2281 was used to measure the level of expression of PARP1 in four different human ovarian and pancreatic tumor models (SKOV3, MIA PaCa-2, PANC-1 and A2780). The SUV_{max} obtained by PET imaging of each of the four tumor types correlated with data for the expression of PARP1 that was obtained by Western blot analysis of cell lysates, although it should be noted that the complete ^{18}F-TCO-tetrazine-AZD2281 radiotracer was administered after the TCO/tetrazine reaction had taken place [101]. The next step will be to demonstrate that ^{18}F-TCO can be used in a pretargeting approach and react with tetrazine-AZD2281 *in vivo*.

8. Pharmacokinetic imaging to model physiological parameters of malignant disease

Nuclear medicine imaging to quantify pharmacokinetic parameters can be used to model the pharmacokinetics of a disease model or human patient. This approach, though relevant to the field of oncology, is less well documented compared to neurology, however. Nevertheless, T_1-weighted MRI has been used to measure such parameters as intratumoral transfer constants, rate constants, and volumes for extracellular space [102]. Although the quantification of such parameters has rarely been reported in PET and SPECT imaging, such radiotracers as ^{18}F-FDG, ^{18}F-FMISO and ^{18}F-FDOPA have been used [103-105].

The compartmental model that was developed as a framework to permit the quantification of pharmacokinetic differences between different (patho)physiological compartments [106], has been used extensively in PET imaging to quantify blood flow using ^{15}O-labelled water [107], cerebral glycolytic rate using ^{18}F-FDG [108], cerebral metabolism of radioligands using ^{18}F-FDOPA [109], and cerebral oxygen utilization using ^{15}O-CO, ^{15}O-CO_2, and ^{15}O-O_2 [110]. These methods have not been adopted as standard practice in the clinic, however, probably because of the need for lengthy kinetic scans rather than time-efficient static scans. Even in preclinical studies, the use of pharmacokinetic modelling methods in oncology has not been anywhere near as widespread as in neuroscience.

Despite the slow uptake of pharmacokinetic modelling in the oncology community, kinetic imaging has great potential to provide relevant information regarding the pharmacologic activity of cancer drugs. The potential for clinical application of kinetic imaging in respect to small molecules is greatest, due to their relatively short biological half-lives which would necessitate short acquisition times to continuously acquire images that show dynamic changes in their biodistribution. Nevertheless, Gleisner *et al.* used parametric imaging based on planar scintillation-camera images to analyse the spatial and temporal distributions of ^{111}In-labelled monoclonal antibodies [111], which have much longer biological half-lives compared to small molecules. Parametric imaging can be used to identify anatomical regions with different pharmacokinetics compared to surrounding normal tissue and thus provides a tool to detect and locate sites of pathophysiological kinetic behaviour that is characteristic of malignant disease.

To improve clinical practice, further studies will be needed to explore the potential of kinetic scans using such radiotracers as ^{18}F-FDG or ^{18}F-FMISO [112, 113]. ^{18}F-FMISO has proven application in PET imaging to quantify the levels of tumor hypoxia, though in pancreatic cancer the median SUV_{max} has been reported to be relatively low (2.23) and tumor-to-blood contrast was also relatively poor (1.0-1.5:1) [114]. Nevertheless, Wang *et al*. have used kinetic ^{18}F-FMISO-PET imaging to model the levels of chronic and acute hypoxia in 14 patients with head and neck cancers, while Kelly *et al.* developed this process further to estimate the true intratumoral oxygen level [115-117]. Thus, imaging hypoxia is becoming increasingly important as a biomarker that can be studied to show the temporal effects of anti-cancer drugs on tumor neovasculature [118-120].

9. Future Perspectives

Nuclear imaging using PET and SPECT offers clear and significant advantages over other diagnostics techniques, and can offer a wide range of clinically relevant information regarding the treatment response, radiotracer biodistribution, tumor accumulation, toxicity, and pharmacokinetic parameters [92]. However, numerous challenges still need to be overcome to make nuclear medicine imaging even more useful. The expensive research infrastructure, in particular, makes radiopharmacy a significant logistical challenge. For example, a cyclotron is required for the production of positron emitters, GMP facilities for manufacture of radiotracers, PET/CT and SPECT/CT scanners for image acquisition, an on-site blood sampler and laboratory for analytical testing, and dedicated computing facilities for analysing image data. In addition, these facilities need to be staffed by a highly trained multidisciplinary team that might include a cyclotron operator, radiochemists, radiopharmacists, an imaging technologist, a nuclear medicine physician, and a physicist. In this regard, infrastructure funding is critical to ensure that these specialist personnel are working within close proximity, to enable to use of short half-life positron emitting radionuclides [92].

Biomarkers feature in the FDA's Critical Path Opportunities List due to their potential to accelerate the translational development and clinical approval of medical products (http://www.fda.gov/oc/initiatives/criticalpath/ reports/opp_list. pdf). The Molecular Imaging and Contrast Agent Database administered by the National Center for Biotechnology Information (NCBI) contains a list of 1,444 radiotracers that are available for the detection of a large number of disease biomarkers. Therefore, a wide range of radiotracers for PET and SPECT molecular imaging can be used to accelerate the translational development of anti-cancer drugs by non-invasively measuring their biological and therapeutic effects through the detection of disease biomarkers. However, with so many radiotracers to choose from, the most important consideration in PET and SPECT molecular imaging must be the selection of the correct radiotracer that measures the most relevant biomarker and provides a valuable surrogate for the robust determination of the delivery, therapeutic efficacy and off-target toxicity of anti-cancer drugs.

The authors have no conflicts of interest to disclose.

Financial Support: This research was supported by CRUK, the CRUK/MRC Oxford Institute for Radiation Oncology, and the CRUK/EPSRC Cancer Imaging Centre in Oxford

10. References

[1] Roentgen WC. [On a new kind of ray (first report)]. Munch Med Wochenschr. 1959;101:1237-9.
[2] Pomper MG. Can small animal imaging accelerate drug development? Journal of cellular biochemistry Supplement. 2002;39:211-20.
[3] Conti PS, McEwan AJ, Pomper MG. Molecular imaging: the future of modern medicine. J Nucl Med. 2008;49(6):16N-20N.
[4] Cherry SR. Multimodality imaging: beyond PET/CT and SPECT/CT. Seminars in nuclear medicine. 2009;39(5):348-53.
[5] Cornelissen B, McLarty K, Kersemans V, Reilly RM. The level of insulin growth factor-1 receptor expression is directly correlated with the tumor uptake of (111)In-IGF-1(E3R) in vivo and the clonogenic survival of breast cancer cells exposed in vitro to trastuzumab (Herceptin). Nucl Med Biol. 2008;35(6):645-53.
[6] Cornelissen B, Thonissen T, Kersemans V, Van De Wiele C, Lahorte C, Dierckx RA, *et. al.* Influence of farnesyl transferase inhibitor treatment on epidermal growth factor receptor status. Nucl Med Biol. 2004;31(6):679-89.
[7] Poot AJ, Slobbe P, Hendrikse NH, Windhorst AD, van Dongen GA. Imaging of TKI-target interactions for personalized cancer therapy. Clinical pharmacology and therapeutics. 2013;93(3):239-41.
[8] Lahorte CM, Vanderheyden JL, Steinmetz N, Van de Wiele C, Dierckx RA, Slegers G. Apoptosis-detecting radioligands: current state of the art and future perspectives. European journal of nuclear medicine and molecular imaging. 2004;31(6):887-919.
[9] Woolf DK, Beresford M, Li SP, Dowsett M, Sanghera B, Wong WL, *et. al.* Evaluation of FLT-PET-CT as an imaging biomarker of proliferation in primary breast cancer. British journal of cancer. 2014;110(12):2847-54.
[10] Temma T, Hanaoka H, Yonezawa A, Kondo N, Sano K, Sakamoto T, *et. al.* Investigation of a MMP-2 activity-dependent anchoring probe for nuclear imaging of cancer. PloS one. 2014;9(7):e102180.
[11] Liu Z, Liu H, Ma T, Sun X, Shi J, Jia B, *et. al.* Integrin alphavbeta6-Targeted SPECT Imaging for Pancreatic Cancer Detection. J Nucl Med. 2014;55(6):989-94.
[12] Cornelissen B, Kersemans V, Darbar S, Thompson J, Shah K, Sleeth K, *et. al.* Imaging DNA damage in vivo using gammaH2AX-targeted immunoconjugates. Cancer research. 2011;71(13):4539-49.
[13] Yamane T, Takaoka A, Kita M, Imai Y, Senda M. 18F-FLT PET performs better than 18F-FDG PET in differentiating malignant uterine corpus tumors from benign leiomyoma. Annals of nuclear medicine. 2012;26(6):478-84.
[14] Huang C, McConathy J. Radiolabeled amino acids for oncologic imaging. J Nucl Med. 2013;54(7):1007-10.
[15] Neves AA, Brindle KM. Imaging cell death. Journal of nuclear medicine : official publication, Society of Nuclear Medicine. 2014;55(1):1-4.
[16] Blankenberg FG. In vivo detection of apoptosis. J Nucl Med. 2008;49 Suppl 2:81S-95S.
[17] Fushiki H, Murakami Y, Miyoshi S, Nishimura S. PET Imaging for Tyrosine Kinase Inhibitor (TKI) Biodistribution in Mice. Methods Mol Biol. 2015;1219:199-206.
[18] Marquez BV, Ikotun OF, Parry JJ, Rogers BE, Meares CF, Lapi SE. Development of a Radiolabeled Irreversible Peptide Ligand for PET Imaging of Vascular Endothelial Growth Factor. J Nucl Med. 2014;55(6):1029-34.

[19] Hood JD, Cheresh DA. Role of integrins in cell invasion and migration. Nat Rev Cancer. 2002;2(2):91-100.
[20] Liu C, Huang H, Wang C, Kong Y, Zhang H. Involvement of ephrin receptor A4 in pancreatic cancer cell motility and invasion. Oncology letters. 2014;7(6):2165-9.
[21] Kim EM, Park EH, Cheong SJ, Lee CM, Kim DW, Jeong HJ, *et. al.* Characterization, biodistribution and small-animal SPECT of I-125-labeled c-Met binding peptide in mice bearing c-Met receptor tyrosine kinase-positive tumor xenografts. Nucl Med Biol. 2009;36(4):371-8.
[22] Benezra M, Hambardzumyan D, Penate-Medina O, Veach DR, Pillarsetty N, Smith-Jones P, *et. al.* Fluorine-labeled dasatinib nanoformulations as targeted molecular imaging probes in a PDGFB-driven murine glioblastoma model. Neoplasia. 2012;14(12):1132-43.
[23] Kudo T, Ueda M, Konishi H, Kawashima H, Kuge Y, Mukai T, *et. al.* PET imaging of hypoxia-inducible factor-1-active tumor cells with pretargeted oxygen-dependent degradable streptavidin and a novel 18F-labeled biotin derivative. Molecular imaging and biology : MIB : the official publication of the Academy of Molecular Imaging. 2011;13(5):1003-10.
[24] Waerzeggers Y, Ullrich RT, Monfared P, Viel T, Weckesser M, Stummer W, *et. al.* Specific biomarkers of receptors, pathways of inhibition and targeted therapies: clinical applications. Br J Radiol. 2011;84 Spec No 2:S179-95.
[25] Waerzeggers Y, Monfared P, Viel T, Faust A, Kopka K, Schafers M, *et. al.* Specific biomarkers of receptors, pathways of inhibition and targeted therapies: pre-clinical developments. Br J Radiol. 2011;84 Spec No 2:S168-78.
[26] Hanahan D, Weinberg RA. Hallmarks of cancer: the next generation. Cell. 2011;144(5):646-74.
[27] Holland JP, Evans MJ, Rice SL, Wongvipat J, Sawyers CL, Lewis JS. Annotating MYC status with 89Zr-transferrin imaging. Nature medicine. 2012;18(10):1586-91.
[28] Cornelissen B, Able S, Kartsonaki C, Kersemans V, Allen PD, Cavallo F, *et. al.* Imaging DNA Damage Allows Detection of Preneoplasia in the BALB-neuT Model of Breast Cancer. Journal of nuclear medicine : official publication, Society of Nuclear Medicine. 2014;55(12):2026-31.
[29] Willmann JK, van Bruggen N, Dinkelborg LM, Gambhir SS. Molecular imaging in drug development. Nature reviews Drug discovery. 2008;7(7):591-607.
[30] Flamen P, Lerut A, Van Cutsem E, De Wever W, Peeters M, Stroobants S, *et. al.* Utility of positron emission tomography for the staging of patients with potentially operable esophageal carcinoma. Journal of clinical oncology : official journal of the American Society of Clinical Oncology. 2000;18(18):3202-10.
[31] Schillaci O, Simonetti G. Fusion imaging in nuclear medicine--applications of dual-modality systems in oncology. Cancer biotherapy & radiopharmaceuticals. 2004;19(1):1-10.
[32] Almuhaideb A, Papathanasiou N, Bomanji J. 18F-FDG PET/CT imaging in oncology. Annals of Saudi medicine. 2011;31(1):3-13.
[33] Neuner I, Kaffanke JB, Langen KJ, Kops ER, Tellmann L, Stoffels G, *et. al.* Multimodal imaging utilising integrated MR-PET for human brain tumour assessment. European radiology. 2012;22(12):2568-80.
[34] Avram AM. Radioiodine scintigraphy with SPECT/CT: an important diagnostic tool for thyroid cancer staging and risk stratification. Journal of nuclear medicine : official publication, Society of Nuclear Medicine. 2012;53(5):754-64.
[35] Bar-Shalom R, Yefremov N, Guralnik L, Gaitini D, Frenkel A, Kuten A, *et. al.* Clinical performance of PET/CT in evaluation of cancer: additional value for diagnostic imaging and patient management. J Nucl Med. 2003;44(8):1200-9.

[36] Mankoff DA, Pryma DA, Clark AS. Molecular imaging biomarkers for oncology clinical trials. Journal of nuclear medicine : official publication, Society of Nuclear Medicine. 2014;55(4):525-8.
[37] Gerlinger M, Rowan AJ, Horswell S, Larkin J, Endesfelder D, Gronroos E, *et. al.* Intratumor heterogeneity and branched evolution revealed by multiregion sequencing. The New England journal of medicine. 2012;366(10):883-92.
[38] Kang F, Ma W, Ma X, Shao Y, Yang W, Chen X, *et. al.* Propranolol Inhibits Glucose Metabolism and 18F-FDG Uptake of Breast Cancer Through Posttranscriptional Downregulation of Hexokinase-2. Journal of Nuclear Medicine. 2014;55(3):439-45.
[39] Jensen MM, Erichsen KD, Johnbeck CB, Bjorkling F, Madsen J, Jensen PB, *et. al.* [18F]FDG and [18F]FLT positron emission tomography imaging following treatment with belinostat in human ovary cancer xenografts in mice. BMC Cancer. 2013;13(1):168.
[40] Munk Jensen M, Erichsen KD, Björkling F, Madsen J, Jensen PB, Sehested M, *et. al.* Imaging of Treatment Response to the Combination of Carboplatin and Paclitaxel in Human Ovarian Cancer Xenograft Tumors in Mice Using FDG and FLT PET. PLoS ONE. 2013;8(12):e85126.
[41] Lheureux S, Lecerf C, Briand M, Louis M-H, Dutoit S, Jebahi A, *et. al.* 18F-FDG Is a Surrogate Marker of Therapy Response and Tumor Recovery after Drug Withdrawal during Treatment with a Dual PI3K/mTOR Inhibitor in a Preclinical Model of Cisplatin-Resistant Ovarian Cancer. Translational Oncology. 2013;6(5):586-IN7.
[42] Keen H, Ricketts S-A, Maynard J, Logie A, Odedra R, Shannon A, *et. al.* Examining Changes in [18 F]FDG and [18 F]FLT Uptake in U87-MG Glioma Xenografts as Early Response Biomarkers to Treatment with the Dual mTOR1/2 Inhibitor AZD8055. Molecular Imaging and Biology. 2014;16(3):421-30.
[43] Vergez S, Delord J-P, Thomas F, Rochaix P, Caselles O, Filleron T, *et. al.* Preclinical and Clinical Evidence that Deoxy-2-[18F]fluoro-D-glucose Positron Emission Tomography with Computed Tomography Is a Reliable Tool for the Detection of Early Molecular Responses to Erlotinib in Head and Neck Cancer. Clinical Cancer Research. 2010;16(17):4434-45.
[44] Brepoels L, De Saint-Hubert M, Stroobants S, Verhoef G, Balzarini J, Mortelmans L, *et. al.* Dose-response relationship in cyclophosphamide-treated B-cell lymphoma xenografts monitored with [18F]FDG PET. European Journal of Nuclear Medicine and Molecular Imaging. 2010;37(9):1688-95.
[45] Song S, Xiong C, Lu W, Ku G, Huang G, Li C. Apoptosis Imaging Probe Predicts Early Chemotherapy Response in Preclinical Models: A Comparative Study with 18F-FDG PET. Journal of Nuclear Medicine. 2013;54(1):104-10.
[46] Mudd S, Voorbach M, Reuter D, Tapang P, Hickson J, Refici-Buhr M, *et. al.* FDG-PET as a pharmacodynamic biomarker for early assessment of treatment response to linifanib (ABT-869) in a non-small cell lung cancer xenograft model. Cancer Chemotherapy and Pharmacology. 2012;69(6):1669-72.
[47] Warburg O, Wind F, Negelein E. The Metabolism of Tumors in the Body. The Journal of general physiology. 1927;8(6):519-30.
[48] Papac RJ. Origins of cancer therapy. The Yale journal of biology and medicine. 2001;74(6):391-8.
[49] DeVita VT, Jr., Chu E. A history of cancer chemotherapy. Cancer research. 2008;68(21):8643-53.
[50] Contractor KB, Aboagye EO. Monitoring Predominantly Cytostatic Treatment Response with 18F-FDG PET. Journal of Nuclear Medicine. 2009;50(Suppl 1):97S-105S.

[51] Jensen MM, Erichsen KD, Johnbeck CB, Bjorkling F, Madsen J, Jensen PB, *et. al.* [18F]FDG and [18F]FLT positron emission tomography imaging following treatment with belinostat in human ovary cancer xenografts in mice. BMC Cancer. 2013;13:168.
[52] Alvarez JV, Belka GK, Pan TC, Chen CC, Blankemeyer E, Alavi A, *et. al.* Oncogene Pathway Activation in Mammary Tumors Dictates FDG-PET Uptake. Cancer research. 2014;74(24):7583-98.
[53] Scott AM, Wolchok JD, Old LJ. Antibody therapy of cancer. Nature reviews Cancer. 2012;12(4):278-87.
[54] Murphy CG, Modi S. HER2 breast cancer therapies: a review. Biologics : targets & therapy. 2009;3:289-301.
[55] Goel HL, Mercurio AM. VEGF targets the tumour cell. Nature reviews Cancer. 2013;13(12):871-82.
[56] Chari RV, Miller ML, Widdison WC. Antibody-drug conjugates: an emerging concept in cancer therapy. Angew Chem Int Ed Engl. 2014;53(15):3796-827.
[57] Goldenberg MM. Trastuzumab, a recombinant DNA-derived humanized monoclonal antibody, a novel agent for the treatment of metastatic breast cancer. Clinical therapeutics. 1999;21(2):309-18.
[58] Beylergil V, Morris PG, Smith-Jones PM, Modi S, Solit D, Hudis CA, *et. al.* Pilot study of 68Ga-DOTA-F(ab')2-trastuzumab in patients with breast cancer. Nucl Med Commun. 2013;34(12):1157-65.
[59] Dijkers EC, Oude Munnink TH, Kosterink JG, Brouwers AH, Jager PL, de Jong JR, *et. al.* Biodistribution of 89Zr-trastuzumab and PET imaging of HER2-positive lesions in patients with metastatic breast cancer. Clinical pharmacology and therapeutics. 2010;87(5):586-92.
[60] Lub-de Hooge MN, Kosterink JG, Perik PJ, Nijnuis H, Tran L, Bart J, *et. al.* Preclinical characterisation of 111In-DTPA-trastuzumab. Br J Pharmacol. 2004;143(1):99-106.
[61] Oude Munnink TH, Korte MA, Nagengast WB, Timmer-Bosscha H, Schroder CP, Jong JR, *et. al.* (89)Zr-trastuzumab PET visualises HER2 downregulation by the HSP90 inhibitor NVP-AUY922 in a human tumour xenograft. Eur J Cancer. 2010;46(3):678-84.
[62] Perik PJ, Lub-De Hooge MN, Gietema JA, van der Graaf WT, de Korte MA, Jonkman S, *et. al.* Indium-111-labeled trastuzumab scintigraphy in patients with human epidermal growth factor receptor 2-positive metastatic breast cancer. J Clin Oncol. 2006;24(15):2276-82.
[63] Tamura K, Kurihara H, Yonemori K, Tsuda H, Suzuki J, Kono Y, *et. al.* 64Cu-DOTA-trastuzumab PET imaging in patients with HER2-positive breast cancer. J Nucl Med. 2013;54(11):1869-75.
[64] Dijkers EC, Kosterink JG, Rademaker AP, Perk LR, van Dongen GA, Bart J, *et. al.* Development and characterization of clinical-grade 89Zr-trastuzumab for HER2/neu immunoPET imaging. J Nucl Med. 2009;50(6):974-81.
[65] Janjigian YY, Viola-Villegas N, Holland JP, Divilov V, Carlin SD, Gomes-DaGama EM, *et. al.* Monitoring afatinib treatment in HER2-positive gastric cancer with 18F-FDG and 89Zr-trastuzumab PET. J Nucl Med. 2013;54(6):936-43.
[66] McLarty K, Cornelissen B, Cai Z, Scollard DA, Costantini DL, Done SJ, *et. al.* Micro-SPECT/CT with 111In-DTPA-pertuzumab sensitively detects trastuzumab-mediated HER2 downregulation and tumor response in athymic mice bearing MDA-MB-361 human breast cancer xenografts. J Nucl Med. 2009;50(8):1340-8.
[67] Smith-Jones PM, Solit D, Afroze F, Rosen N, Larson SM. Early tumor response to Hsp90 therapy using HER2 PET: comparison with 18F-FDG PET. J Nucl Med. 2006;47(5):793-6.

[68] McLarty K, Cornelissen B, Scollard DA, Done SJ, Chun K, Reilly RM. Associations between the uptake of 111In-DTPA-trastuzumab, HER2 density and response to trastuzumab (Herceptin) in athymic mice bearing subcutaneous human tumour xenografts. European journal of nuclear medicine and molecular imaging. 2009;36(1):81-93.
[69] Greish K. Enhanced permeability and retention (EPR) effect for anticancer nanomedicine drug targeting. Methods Mol Biol. 2010;624:25-37.
[70] McLarty K, Fasih A, Scollard DA, Done SJ, Vines DC, Green DE, *et. al.* 18F-FDG small-animal PET/CT differentiates trastuzumab-responsive from unresponsive human breast cancer xenografts in athymic mice. J Nucl Med. 2009;50(11):1848-56.
[71] Behr TM, Behe M, Wormann B. Trastuzumab and breast cancer. The New England journal of medicine. 2001;345(13):995-6.
[72] Perik PJ, de Korte MA, van Veldhuisen DJ, Gietema JA, Sleijfer DT, de Vries EG. Cardiotoxicity associated with the use of trastuzumab in breast cancer patients. Expert review of anticancer therapy. 2007;7(12):1763-71.
[73] de Geus-Oei LF, Mavinkurve-Groothuis AM, Bellersen L, Gotthardt M, Oyen WJ, Kapusta L, *et. al.* Scintigraphic techniques for early detection of cancer treatment-induced cardiotoxicity. J Nucl Med. 2011;52(4):560-71.
[74] Milano GA, Serres E, Ferrero JM, Ciccolini J. Trastuzumab-Induced Cardiotoxicity: Is it a Personalized Risk? Current drug targets. 2014;15(13):1200-4.
[75] Stollman TH, Ruers TJ, Oyen WJ, Boerman OC. New targeted probes for radioimaging of angiogenesis. Methods. 2009;48(2):188-92.
[76] O'Connor JP, Carano RA, Clamp AR, Ross J, Ho CC, Jackson A, *et. al.* Quantifying antivascular effects of monoclonal antibodies to vascular endothelial growth factor: insights from imaging. Clinical cancer research : an official journal of the American Association for Cancer Research. 2009;15(21):6674-82.
[77] Christoforidis JB, Carlton MM, Knopp MV, Hinkle GH. PET/CT imaging of I-124-radiolabeled bevacizumab and ranibizumab after intravitreal injection in a rabbit model. Investigative ophthalmology & visual science. 2011;52(8):5899-903.
[78] Chang AJ, Sohn R, Lu ZH, Arbeit JM, Lapi SE. Detection of rapalog-mediated therapeutic response in renal cancer xenografts using (6)(4)Cu-bevacizumab immunoPET. PloS one. 2013;8(3):e58949.
[79] Golestani R, Zeebregts CJ, Terwisscha van Scheltinga AG, Lub-de Hooge MN, van Dam GM, Glaudemans AW, *et. al.* Feasibility of vascular endothelial growth factor imaging in human atherosclerotic plaque using (89)Zr-bevacizumab positron emission tomography. Molecular imaging. 2013;12(4):235-43.
[80] Hong DS, Garrido-Laguna I, Ekmekcioglu S, Falchook GS, Naing A, Wheler JJ, *et. al.* Dual inhibition of the vascular endothelial growth factor pathway: a phase 1 trial evaluating bevacizumab and AZD2171 (cediranib) in patients with advanced solid tumors. Cancer. 2014;120(14):2164-73.
[81] Hosseinimehr SJ, Orlova A, Tolmachev V. Preparation and in vitro evaluation of 111In-CHX-A"-DTPA-labeled anti-VEGF monoclonal antibody bevacizumab. Human antibodies. 2010;19(4):107-11.
[82] Desar IM, Stillebroer AB, Oosterwijk E, Leenders WP, van Herpen CM, van der Graaf WT, *et. al.* 111In-bevacizumab imaging of renal cell cancer and evaluation of neoadjuvant treatment with the vascular endothelial growth factor receptor inhibitor sorafenib. J Nucl Med. 2010;51(11):1707-15.
[83] Scheer MG, Stollman TH, Boerman OC, Verrijp K, Sweep FC, Leenders WP, *et. al.* Imaging liver metastases of colorectal cancer patients with radiolabelled bevacizumab: Lack of correlation with VEGF-A expression. Eur J Cancer. 2008;44(13):1835-40.

[84] Stollman TH, Scheer MG, Leenders WP, Verrijp KC, Soede AC, Oyen WJ, *et. al.* Specific imaging of VEGF-A expression with radiolabeled anti-VEGF monoclonal antibody. International journal of cancer Journal international du cancer. 2008;122(10):2310-4.
[85] Stollman TH, Scheer MG, Franssen GM, Verrijp KN, Oyen WJ, Ruers TJ, *et. al.* Tumor accumulation of radiolabeled bevacizumab due to targeting of cell- and matrix-associated VEGF-A isoforms. Cancer biotherapy & radiopharmaceuticals. 2009;24(2):195-200.
[86] Heskamp S, Boerman OC, Molkenboer-Kuenen JD, Sweep FC, Geurts-Moespot A, Engelhardt MS, *et. al.* Cetuximab Reduces the Accumulation of Radiolabeled Bevacizumab in Cancer Xenografts without Decreasing VEGF Expression. Molecular pharmaceutics. 2014.
[87] Terry SY, Abiraj K, Lok J, Gerrits D, Franssen GM, Oyen WJ, *et. al.* Can 111In-RGD2 monitor response to therapy in head and neck tumor xenografts? Journal of nuclear medicine : official publication, Society of Nuclear Medicine. 2014;55(11):1849-55.
[88] Rosier A, Dupont P, Peuskens J, Bormans G, Vandenberghe R, Maes M, *et. al.* Visualisation of loss of 5-HT2A receptors with age in healthy volunteers using [18F]altanserin and positron emission tomographic imaging. Psychiatry research. 1996;68(1):11-22.
[89] Dimasi JA. Risks in new drug development: approval success rates for investigational drugs. Clinical pharmacology and therapeutics. 2001;69(5):297-307.
[90] Gomes CM, Abrunhosa AJ, Ramos P, Pauwels EK. Molecular imaging with SPECT as a tool for drug development. Adv Drug Deliv Rev. 2011;63(7):547-54.
[91] Fischman AJ, Alpert NM, Rubin RH. Pharmacokinetic imaging: a noninvasive method for determining drug distribution and action. Clinical pharmacokinetics. 2002;41(8):581-602.
[92] van der Veldt AA, Smit EF, Lammertsma AA. Positron Emission Tomography as a Method for Measuring Drug Delivery to Tumors in vivo: The Example of [(11)C]docetaxel. Frontiers in oncology. 2013;3:208.
[93] van der Veldt AA, Hendrikse NH, Smit EF, Mooijer MP, Rijnders AY, Gerritsen WR, *et. al.* Biodistribution and radiation dosimetry of 11C-labelled docetaxel in cancer patients. European journal of nuclear medicine and molecular imaging. 2010;37(10):1950-8.
[94] van der Veldt AA, Lubberink M, Greuter HN, Comans EF, Herder GJ, Yaqub M, *et. al.* Absolute quantification of [(11)C]docetaxel kinetics in lung cancer patients using positron emission tomography. Clin Cancer Res. 2011;17(14):4814-24.
[95] Goldenberg DM, Chang CH, Rossi EA, J W, McBride, Sharkey RM. Pretargeted molecular imaging and radioimmunotherapy. Theranostics. 2012;2(5):523-40.
[96] Knight JC, Cornelissen B. Bioorthogonal chemistry: implications for pretargeted nuclear (PET/SPECT) imaging and therapy. American journal of nuclear medicine and molecular imaging. 2014;4(2):96-113.
[97] Stickney DR, Anderson LD, Slater JB, Ahlem CN, Kirk GA, Schweighardt SA, *et. al.* Bifunctional antibody: a binary radiopharmaceutical delivery system for imaging colorectal carcinoma. Cancer research. 1991;51(24):6650-5.
[98] Chang CH, Sharkey RM, Rossi EA, Karacay H, McBride W, Hansen HJ, *et. al.* Molecular advances in pretargeting radioimunotherapy with bispecific antibodies. Molecular cancer therapeutics. 2002;1(7):553-63.
[99] Keliher EJ, Reiner T, Turetsky A, Hilderbrand SA, Weissleder R. High-yielding, two-step 18F labeling strategy for 18F-PARP1 inhibitors. ChemMedChem. 2011;6(3):424-7.
[100] Reiner T, Earley S, Turetsky A, Weissleder R. Bioorthogonal small-molecule ligands for PARP1 imaging in living cells. Chembiochem : a European journal of chemical biology. 2010;11(17):2374-7.

[101] Reiner T, Lacy J, Keliher EJ, Yang KS, Ullal A, Kohler RH, *et. al.* Imaging therapeutic PARP inhibition in vivo through bioorthogonally developed companion imaging agents. Neoplasia. 2012;14(3):169-77.
[102] Bergamino M, Bonzano L, Levrero F, Mancardi GL, Roccatagliata L. A review of technical aspects of T1-weighted dynamic contrast-enhanced magnetic resonance imaging (DCE-MRI) in human brain tumors. Phys Med. 2014;30(6):635-43.
[103] Zhang H, Tan S, Chen W, Kligerman S, Kim G, D'Souza WD, *et. al.* Modeling pathologic response of esophageal cancer to chemoradiation therapy using spatial-temporal 18F-FDG PET features, clinical parameters, and demographics. International journal of radiation oncology, biology, physics. 2014;88(1):195-203.
[104] Chang JH, Wada M, Anderson NJ, Lim Joon D, Lee ST, Gong SJ, *et. al.* Hypoxia-targeted radiotherapy dose painting for head and neck cancer using (18)F-FMISO PET: a biological modeling study. Acta Oncol. 2013;52(8):1723-9.
[105] Shoghi-Jadid K, Huang SC, Stout DB, Yee RE, Yeh EL, Farahani KF, *et. al.* Striatal kinetic modeling of FDOPA with a cerebellar-derived constraint on the distribution of volume of 30MFD: a PET investigation using non-human primates. Journal of cerebral blood flow and metabolism : official journal of the International Society of Cerebral Blood Flow and Metabolism. 2000;20(7):1134-48.
[106] Watabe H, Ikoma Y, Kimura Y, Naganawa M, Shidahara M. PET kinetic analysis--compartmental model. Annals of nuclear medicine. 2006;20(9):583-8.
[107] Kety SS. The theory and applications of the exchange of inert gas at the lungs and tissues. Pharmacological reviews. 1951;3(1):1-41.
[108] Reivich M, Kuhl D, Wolf A, Greenberg J, Phelps M, Ido T, *et. al.* The [18F]fluorodeoxyglucose method for the measurement of local cerebral glucose utilization in man. Circulation research. 1979;44(1):127-37.
[109] Endres CJ, DeJesus OT, Uno H, Doudet DJ, Nickles JR, Holden JE. Time profile of cerebral [18F]6-fluoro-L-DOPA metabolites in nonhuman primate: implications for the kinetics of therapeutic L-DOPA. Frontiers in bioscience : a journal and virtual library. 2004;9:505-12.
[110] Mintun MA, Raichle ME, Martin WR, Herscovitch P. Brain oxygen utilization measured with O-15 radiotracers and positron emission tomography. Journal of nuclear medicine : official publication, Society of Nuclear Medicine. 1984;25(2):177-87.
[111] Gleisner KS, Nickel M, Linden O, Erlandsson K, Wingardh K, Strand SE. Parametric images of antibody pharmacokinetics based on serial quantitative whole-body imaging and blood sampling. Journal of nuclear medicine : official publication, Society of Nuclear Medicine. 2007;48(8):1369-78.
[112] Koh WJ, Rasey JS, Evans ML, Grierson JR, Lewellen TK, Graham MM, *et. al.* Imaging of hypoxia in human tumors with [F-18]fluoromisonidazole. International journal of radiation oncology, biology, physics. 1992;22(1):199-212.
[113] Rasey JS, Koh WJ, Evans ML, Peterson LM, Lewellen TK, Graham MM, *et. al.* Quantifying regional hypoxia in human tumors with positron emission tomography of [18F]fluoromisonidazole: a pretherapy study of 37 patients. International journal of radiation oncology, biology, physics. 1996;36(2):417-28.
[114] Segard T, Robins PD, Yusoff IF, Ee H, Morandeau L, Campbell EM, *et. al.* Detection of hypoxia with 18F-fluoromisonidazole (18F-FMISO) PET/CT in suspected or proven pancreatic cancer. Clinical nuclear medicine. 2013;38(1):1-6.
[115] Wang K, Yorke E, Nehmeh SA, Humm JL, Ling CC. Modeling acute and chronic hypoxia using serial images of 18F-FMISO PET. Medical physics. 2009;36(10):4400-8.

[116] Wang W, Georgi JC, Nehmeh SA, Narayanan M, Paulus T, Bal M, *et. al.* Evaluation of a compartmental model for estimating tumor hypoxia via FMISO dynamic PET imaging. Physics in medicine and biology. 2009;54(10):3083-99.
[117] Kelly CJ, Brady M. A model to simulate tumour oxygenation and dynamic [18F]-Fmiso PET data. Physics in medicine and biology. 2006;51(22):5859-73.
[118] Oehler C, O'Donoghue JA, Russell J, Zanzonico P, Lorenzen S, Ling CC, *et. al.* 18F-fluromisonidazole PET imaging as a biomarker for the response to 5,6-dimethylxanthenone-4-acetic acid in colorectal xenograft tumors. Journal of nuclear medicine : official publication, Society of Nuclear Medicine. 2011;52(3):437-44.
[119] Kaneta T, Takai Y, Iwata R, Hakamatsuka T, Yasuda H, Nakayama K, *et. al.* Initial evaluation of dynamic human imaging using 18F-FRP170 as a new PET tracer for imaging hypoxia. Annals of nuclear medicine. 2007;21(2):101-7.
[120] Murakami M, Zhao S, Zhao Y, Chowdhury NF, Yu W, Nishijima K, *et. al.* Evaluation of changes in the tumor microenvironment after sorafenib therapy by sequential histology and 18F-fluoromisonidazole hypoxia imaging in renal cell carcinoma. International journal of oncology. 2012;41(5):1593-600.
[121] Keunen O, Taxt T, Gruner R, Lund-Johansen M, Tonn JC, Pavlin T, *et. al.* Multimodal imaging of gliomas in the context of evolving cellular and molecular therapies. Advanced drug delivery reviews. 2014;76:98-115.

Table 1: Features of SPECT and PET

PET	**SPECT**
Uses positron emitting radionuclides with short half-life isotopes such as carbon-11, oxygen-15 or fluorine-18	Uses the direct gamma radiations emitted by long half-life isotopes such as technetium-99m or iodine-123
High sensitivity (10^{-11}–10^{-12} mol/l) and limited spatial resolution (5–10 mm)	Good sensitivity (10^{-10}–10^{-11} mol/l) and limited spatial resolution (7–15 mm)
Production of radioisotopes is expensive and requires the proximity of a cyclotron	Well established, widely used, cheaper than PET
Molecular imaging of single targets such as receptors, enzymes or proteins	Simultaneously image several radiotracers (differentiated by their energy)
Biodistribution of radiotracers depends on the blood-brain barrier, trapping of enzyme substrates, cell surface internalization, protein binding and metabolism	

Adapted from [121]

Figure 1: Figure 1: Monitoring the tumor response to linifanib with ^{18}F-FDG-PET imaging. *(A) Percentage baseline of the SUV for PET imaging taken at days -1, 1, 3, and 7 showing ^{18}F-FDG uptake in a murine model of human non-small cell lung cancer (Calu-6) treated with vehicle or linifanib (B) PET images at days -1 and 7 showing ^{18}F-FDG uptake in a murine model of human non-small cell lung cancer (Calu-6) treated with vehicle or linifanib. Reproduced from [46]*

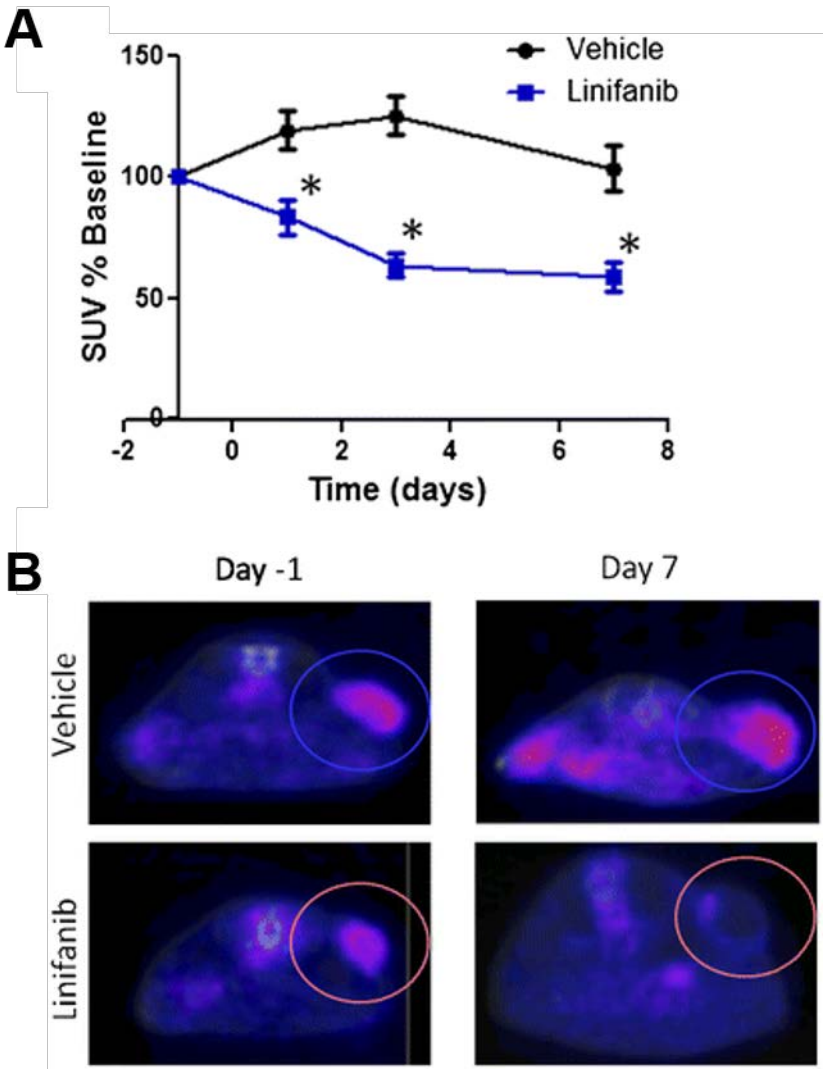

Figure 2: A microdosing to show the biodistribution of ^{11}C-docetaxel in rats. *(A) PET image showing the biodistribution of [^{11}C]docetaxel in a rat. (B) Standardized uptake values of [^{11}C]docetaxel in organs as obtained from dissection studies. Adapted from [92]*

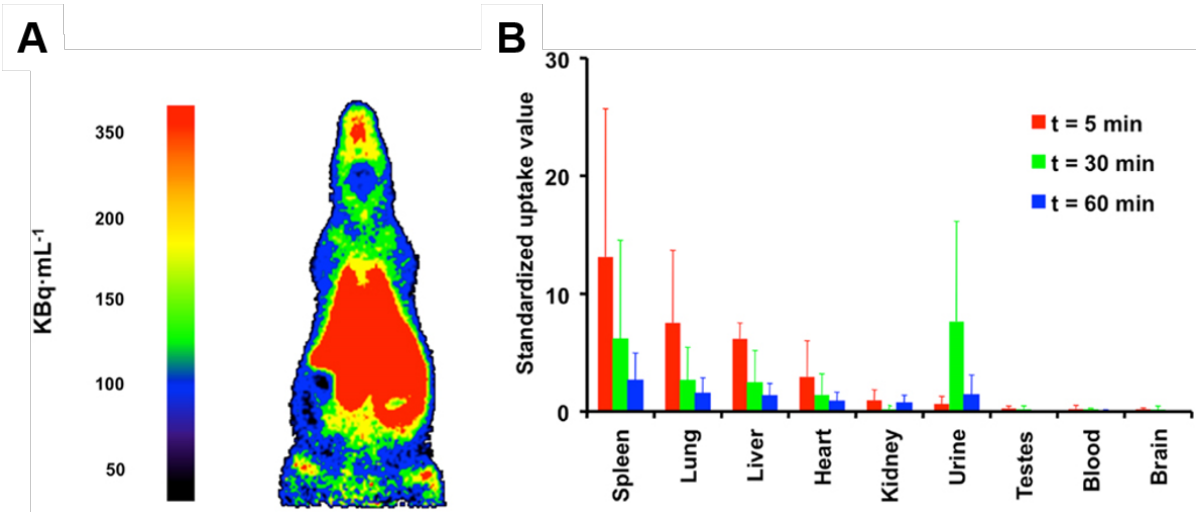

Figure 3: In vitro and in vivo validation of a pre-targeting approach based on biorthogonally-labelled AZD2281 (Olaparib). *(A) TCO-AZD2281 reacted with Texas Red-Tetrazine and colocalized with (B) anti-PARP1 monoclonal antibody staining. Scale Bar: 20 µm. Representative PET-CT images of A2780 tumors (high PARP levels) using ^{18}F-BO (C) before and (D) after treatment with AZD2281. Adapted from [100, 101]*